Optics Letters

Efficient point-by-point Bragg grating inscription in sapphire fiber using femtosecond laser filaments

Xizhen Xu,[1,2] Jun He,[1,2,*] Jia He,[1,2] Baijie Xu,[1,2] Runxiao Chen,[1,2] Ying Wang,[1,2] Yatao Yang,[3] and Yiping Wang[1,2]

[1]Key Laboratory of Optoelectronic Devices and Systems of Ministry of Education/Guangdong Province, College of Physics and Optoelectronic Engineering, Shenzhen University, Shenzhen 518060, China
[2]Shenzhen Key Laboratory of Photonic Devices and Sensing Systems for Internet of Things, Guangdong and Hong Kong Joint Research Centre for Optical Fibre Sensors, Shenzhen University, Shenzhen 518060, China
[3]College of Electronics and Information Engineering, Shenzhen University, Shenzhen 518060, China
*Corresponding author: hejun07@szu.edu.cn

Received 29 March 2021; revised 12 May 2021; accepted 12 May 2021; posted 12 May 2021 (Doc. ID 426407); published 25 May 2021

Sapphire fiber Bragg gratings (SFBGs) inscribed by using femtosecond laser point-by-point (PbP) technology typically have an extremely low reflectivity due to the limited cross-sectional area of refractive index modulations (RIMs) created in sapphire fiber. Hence, we propose and experimentally demonstrate a filamentation process for fabricating PbP SFBGs. This approach provides an efficient method for producing SFBGs at various Bragg wavelengths with a higher reflectivity, since the filament tracks could enlarge the cross-sectional area of RIMs. The influences of the pulse energy and the focal depth on the generation and morphology of the filament tracks were studied, and after optimizing these parameters, high-quality filament tracks with a length of 90 μm and a width of 1.4 μm were produced into sapphire fiber with a diameter of 100 μm. These filament tracks were precisely assembled in sapphire fiber, generating an SFBG with a reflectivity of 2.3%. The total fabrication time for this SFBG only requires ~1.1 s. Subsequently, a wavelength-division-multiplexed (WDM) SFBG array consisting of five SFBGs was efficiently constructed. Moreover, the high-temperature response of the SFBG array was investigated and the experimental results showed that the SFBG array can withstand a high temperature of 1600°C. Such a WDM SFBG array could serve as quasi-distributed high-temperature sensor which will be promising in many areas, i.e., metallurgical, chemical, and aviation industries.

https://doi.org/10.1364/OL.426407

Single-crystal sapphire fibers have a high melting temperature of ~2045°C and hence could be developed for fabricating various high-temperature sensors. As important temperature sensing elements, sapphire fiber Bragg gratings (SFBGs) can be used in many fields, including metallurgical, chemical, and aviation industries [1–6]. To date, three different methods, i.e., the scanning-beam phase mask method [1,2], the Talbot interferometer method [3], and the direct writing technique [4–6], have been reported for creating Bragg gratings in single-crystal sapphire fibers by using a femtosecond laser. An SFBG with a high reflectivity can be fabricated by a femtosecond laser scanning-beam phase mask technique due to a large area of refractive index modulations (RIMs) created by using this method [2]. The fixed period of the phase mask hampers the fabrication of a wavelength-division-multiplexed (WDM) SFBG array. Moreover, a WDM SFBG array could be created flexibly by a femtosecond laser Talbot interferometer [3]. Recently, a femtosecond laser point-by-point (PbP) technique was reported for creating a WDM SFBG array [4]. However, the extremely low reflectivity (i.e., ~0.6%) of SFBGs inscribed using this method can be achieved due to the limited area of RIMs induced by a single pulse. To overcome this issue, we reported on the fabrication of SFBGs with a femtosecond laser line-by-line scanning technique, and the SFBG with a reflectivity of 6.3% was obtained [5]. Furthermore, we fabricated multi-layer SFBGs using this method, and the reflectivity can be enhanced to 34.1% since the area of RIMs formed by multi-layer structure is much larger than that formed by single-layer structure [6]. However, this method is time-consuming (i.e., more than dozens of minutes) for fabrication of an SFBG since a single RIM created requires multiple exposures. Hence, it is not efficient to fabricate a WDM SFBG array by use of a femtosecond laser line-by-line scanning technique.

An enlarged area of RIMs induced by a single femtosecond laser pulse could solve this problem. The filament track generated by a single femtosecond pulse could enlarge the area of RIMs efficiently since the filament track has an elongated geometry. The filamentation process was explained by a balance between Kerr self-focusing and defocusing by laser-induced electron plasma. Filamentation was discovered in various optical media, such as air, liquid, glass, and crystal [7–10]. Recently, a filamentation regime resulting in RIMs in single-crystal sapphires was confirmed [11,12]. The filament tracks were found to include two different types of RIMs, i.e., a permanently damaged region and a nonpermanent region. The high-temperature characteristics of the filament tracks induced in sapphire materials have been studied. The permanently damaged region with a high thermal resistance (i.e., 1500°C) can be employed to fabricate type II FBGs. Moreover, it was reported that the femtosecond laser filamentation was introduced for fabricating strong FBGs into silica fibers [13–15]. These results demonstrate that the filament tracks generated by femtosecond laser pulses can be employed to create SFBGs with the high thermal resistance.

In this Letter, we report for the first time, to the best of our knowledge, a new method for fabricating PbP FBGs in sapphire fibers using the femtosecond laser filamentation. We studied the effects of the pulse energy and the focal depth on generation and morphology of the filament tracks. After optimizing these parameters, an elongated filament track can be created into a sapphire fiber using a single pulse. Hence, the area of RIMs created by this method was much larger than that created by a conventional PbP inscription method. Then an SFBG was successfully produced based on these filament tracks. In addition, a WDM array consisting of five SFBGs was constructed efficiently. Furthermore, we tested the high-temperature response of the fabricated SFBG array. The results show that these SFBGs could withstand a high temperature of 1600°C.

The principle and experimental setup used for the formation of filament track Bragg gratings into sapphire fibers are exhibited in Fig. 1. A frequency-doubled regenerative amplified Yb:KGW (KGd(WO3)) femtosecond laser (Pharos, Light Conversion) with a central wavelength of 514 nm, a pulse width of 290 fs, a repetition rate of 200 kHz, and a laser spot diameter of 3 mm was employed. The repetition rate of 1 kHz was obtained by using a pulse picker. The conventional PbP FBG was fabricated by using an oil-immersion objective with a high numerical aperture (NA). Nevertheless; such a high NA favors the production of micro-explosion voids and restricts the length of the filament track [15]. Then a Mitutoyo dry objective (100×, NA = 0.70, working distance (WD) = 6 mm) was selected in our experiments. A commercial single-crystal sapphire fiber with a diameter of 100 μm and a refractive index of 1.745 at 1550 nm (MicroMaterials Inc.) was employed to induce filament tracks. Such a sapphire fiber was mounted on a fused silica plate, and one of its flat faces was tuned to be normal to the incident beam. The surface curvature of fiber introduces a cylindrical lens effect to the incident beam leading to astigmatic focusing. In order to solve this problem, a fused silica plate with a thickness of 1 mm was positioned parallel and in near-contact with the sapphire fiber. Refractive index oil ($n \approx 1.745$) was applied to fill the gap between the sapphire fiber and the glass slides. Another silica plate was placed under the sapphire fiber for carrying the sapphire fiber and the refractive index oil. All of them were moved precisely using an assembled 3D translation stage (Aerotech ABL15010, ANT130LZS, and ANT130V-5).

Filamentation occurs as the incident peak power exceeds the critical power of self-focusing. An expression of the critical power for a Gaussian beam is given by $P_{\mathrm{cr}} = 3.77\lambda_0^2/8\pi n_0 n_2$, where 3.77 is a coefficient for a Gaussian beam, λ_0 is the laser pulse wavelength, n_0 and n_2 are the linear and nonlinear refractive indices of the medium, respectively) [10]. Additionally, the linear and nonlinear refractive indices of sapphire (i.e., n_0 and n_2) at the femtosecond laser wavelength (514 nm) are 1.78 and $3.29 \times 10^{-20}\ \mathrm{m^2/W}$ [16]. According to the self-focusing formula, the self-focusing threshold power (P_{cr}) was calculated as 6.77×10^5 W. The corresponding critical energy at a pulse width of 290 fs can be calculated as $E_{\mathrm{cr}} = 1.25\tau P_{\mathrm{cr}} = 0.245$ μJ, where τ is the pulse width [10]. As the femtosecond laser beam contracts spatially at the focal volume, its intensity rises and after a certain time becomes sufficient enough to ionize electrons through multi-photon absorption. The generated free electrons reduce the refractive index and counter-balance self-focusing, leading to a dynamic self-guiding of the pulse in the form of a narrow filament track.

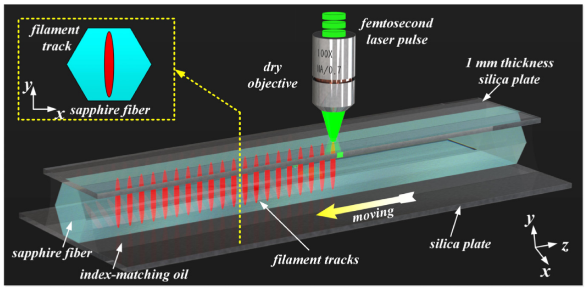

Fig. 1. Experimental setup for PbP SFBGs inscription with a femtosecond laser filamentation. (Inset: schematic of the cross section of the RIM formed by a filament track.)

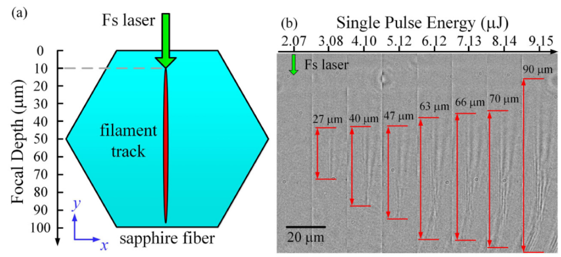

Fig. 2. Filament tracks generated with various pulse energies ranging from 2.07 to 9.15 μJ at a constant focal depth of 10 μm. (a) Schematic of the filament track generated by using a femtosecond laser single pulse. (b) Lateral-view microscope images of the filament tracks.

We studied the effect of laser pulse energy on the generation of filament tracks in a sapphire fiber. As shown in Fig. 2(a), various pulse energies ranging from 2.07 to 9.15 μJ were used to inscribe the filament tracks into the sapphire fiber at the focal depth of 10 μm. All the pulse energies used for this experiment exceed the critical energy. The filament tracks were generated along the direction of femtosecond laser incidence. The lateral-view microscopic images of these filament tracks are shown in Fig. 2(b). The lengths of filament tracks increase with the increasing pulse energies, and the filament track with a maximum length of 90 μm can be obtained at the pulse energy of 9.15 μJ. Moreover, the filament track has become less pronounced at the pulse energy of 2.07 μJ. These results illustrate that increasing the pulse energy is an effective way to improve the length of the filament track.

Subsequently, we studied the effect of the focal depth on the generation and morphology of filament tracks generated in the sapphire fiber. As shown in Fig. 3, the single pulse energy of 9.445 μJ was employed to produce filament tracks into the sapphire fiber at various focal depths ranging from 0 to 60 μm. The lateral-view microscopic images of these filament tracks are shown in Fig. 3. The maximum length of filament tracks of

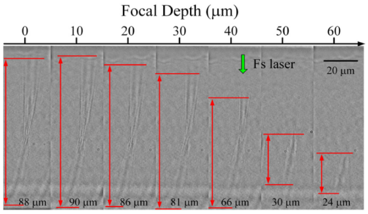

Fig. 3. Lateral-view microscope images of the filament tracks generated with 9.15 μJ pulse energy at various focal depths ranging from 0 to 60 μm.

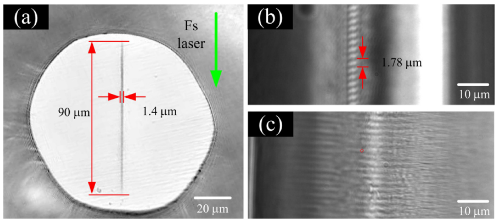

Fig. 4. Microscope images of the SFBG formed by the filament tracks. (a) Cross-sectional view, (b) top view, and (c) lateral view.

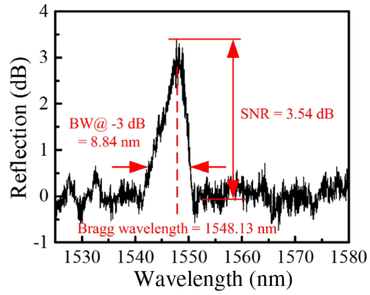

Fig. 5. Reflection spectrum of an SFBG formed by the filament tracks. Note that the reference level of 0 dB corresponds to a reflectivity of ∼1.0%.

90 μm can be obtained at the focal depth of 10 μm. Moreover, the filament track was not straight. Especially, the deviation of the filament track was more obvious as the femtosecond laser pulse propagates over a distance into the sapphire fiber. As in [15], this phenomenon is not observed in the silica fiber. These results indicate that the physical mechanism of filament tracks generated into single-crystal sapphires is complicated and needs further study. Nevertheless, filament tracks can still be precisely assembled inside a sapphire fiber, generating strong Bragg resonances.

Hence, after optimizing these parameters, a filament track with a wide of ∼1 μm and a length of 90 μm has a high aspect ratio. This result indicates that these filament tracks are suitable for forming SFBGs. In order to inscribe the SFBG with a Bragg wavelength in the C-band, the pitch of a fourth-order grating is 1.78 μm as the refractive index of the sapphire fiber is about 1.745 at 1550 nm. In the fabrication process, the moving speed of the sapphire fiber was set to be 1.78 mm/s, and the repetition rate of the laser was 1 kHz, resulting in an SFBG with a grating pitch of 1.78 μm. Moreover, the grating length was 2 mm. Thus, the total fabrication time for this SFBG only requires ∼1.1 s. As shown in Fig. 4(a), the cross section of the sapphire fiber is not circular, but hexagonal. The length and the width of the filament tracks were measured to be 90 and 1.4 μm, respectively. The filament tracks almost traverse the whole section of the sapphire fiber with a diameter of 100 μm. Figures 2(b) and 2(c) show the top-view and lateral-view microscopic images of the SFBG. The spacing of these filament tracks (i.e., grating pitch) was measured to be 1.78 μm.

The reflection spectrum of the SFBG was measured using the setup as in [5] and presented in Fig. 5. It should be noted that the 0 dB corresponds to a reflectivity of ∼1.0% of the polished sapphire fiber end, which was measured in advance and used as a reference. A Bragg wavelength, a −3 dB bandwidth [i.e., full-width at half-maximum, a reflectivity, and a signal-to-noise ratio (SNR) of the SFBG are measured to be 1548.13and 8.84 nm, ∼2.3%, and 3.54 dB, respectively. The reflectivity of the PbP SFBGs formed by the filament tracks is higher than that of conventional PbP SFBGs [4] and close to that of SFBGs inscribed by the line-by-line scanning technique [5]. This result benefits from an enlarged index modulation area.

Furthermore, a WDM SFBG array was fabricated into a 600 mm long sapphire fiber by using filament tracks. Figure 6(a) describes the procedure for fabrication of the array. The fiber was translated along the axis direction (blue line) at a constant speed with a distance of L. Simultaneously, the shutter was opened, and the grating structure was inscribed in these fiber regions. The shutter was closed at the acceleration process (red line), and these fiber regions have no grating structure. The constant moving speeds of 1.76, 1.78, 1.80, 1.82, and 1.84 mm/s were employed to fabricate five SFBGs in different fiber regions. Then an SFBG array includes five 4 mm long SFBGs (i.e., SFBG 1, SFBG 2, SFBG 3, SFBG 4, and SFBG 5) with varying grating pitches Λ of 1.76, 1.78, 1.80, 1.82, and 1.84 μm. The distance between adjacent SFBGs is 20 mm. An optical frequency domain reflectometer (Luna Innovations OBR 4600) was used as a readout system for the SFBG array. A 105/125 μm multimode silica fiber was selected as the lead-in fiber due to its capability of exciting a sufficient number of modes in the sapphire fiber. Figure 6(b) show the reflection spectrum of the SFBG array measured from the A-end. In order to improve the measurement accuracy of the peak wavelengths, the Savitzky–Golay method-based smoothing had already been performed on these reflection spectra. The Bragg wavelengths of SFBG 1, SFBG 2, SFBG 3, SFBG 4, and SFBG 5 were 1534.25, 1548.67, 1566.62, 1583.38, and 1601.16 nm, respectively. Moreover, the reflection peaks were not uniform, but decreased gradually from SFBG1 to SFBG5. This phenomenon is consistent with the reflection spectrum of the SFBG array inscribed by using a femtosecond laser line-by-line scanning technique [5]. It can be explained by the accumulated insertion loss induced by each SFBG and the multimode transmission loss of the sapphire fiber. It can be seen from Fig. 6(b) that the peak reflection of SFBG1 and SFBG2 are −56.368 dB and −56.910 dB, respectively. Hence, the insertion loss can be estimated roughly to be less than 0.5 dB.

The high-temperature response of the WDM SFBG array has been evaluated for temperatures up to 1600 C using the experimental setup and the procedure as in [5,6]. Figure 7(a) displays the reflection spectra of the WDM SFBG array at various temperatures of 11 C, 800 C, and 1600 C. The Bragg wavelengths of SFBGs have redshifts. The complete temperature response of the array from room temperature up to 1600°C is demonstrated

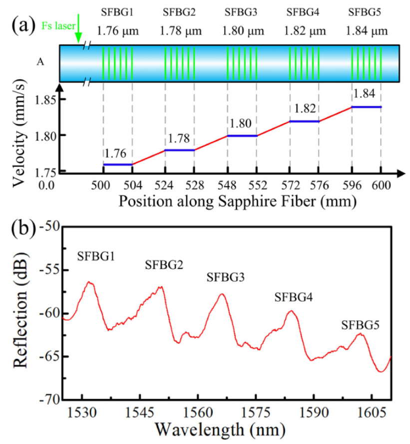

Fig. 6. (a) Fabrication procedure of a serial SFBG array consisting of five SFBGs at different Bragg wavelengths and (b) measured reflection spectrum of the SFBG array.

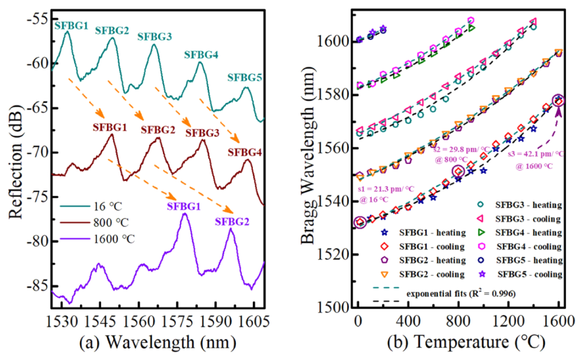

Fig. 7. (a) Evolutions of reflection spectra of the WDM SFBG array at elevated temperatures of 16°C, 800°C, and 1600°C. Hereafter, the spectra are plotted with an offset in the vertical axis for clarity. (b) Bragg wavelengths of the serial SFBG array as functions of the temperature in the case of temperature cycling from 16°C to 1600°C.

in Fig. 7(b). It is obvious that the SFBGs assembled by the filament tracks could withstand a high temperature of 1600°C. Moreover, it can also be observed that the Bragg wavelength of the fabricated SFBG has a nonlinear thermal response, which can be fit with an exponential curve: $\lambda = A + B \cdot e^{(T-C)/D}$. The fitting parameters (i.e., A, B, C, and D) of the heating curve of SFBG1 are 1511.9254, 12.2933, −605.1196, and 1304.9734, respectively. The thermal sensitivities of these SFBGs at various temperatures, i.e., 21.3 pm/°C at 16°C, 29.8 pm/°C at 800°C, and 42.1 pm/°C at 1600°C, were evaluated by applying exponential fits to the measured data, and the results are consistent with the SFBGs created by a femtosecond laser line-by-line scanning technique [5].

In summary, we have demonstrated an efficient method for fabricating PbP SFBGs using femtosecond laser filamentation. The effects of laser pulse energy and focal depth on the formation of filament tracks were experimentally studied, and a filament track with a length of 90 μm and a width of 1.4 μm was successfully generated in a sapphire fiber. Note that the created filament track almost traversed the whole cross section of the sapphire fiber with a diameter of 100 μm. Hence, an enlarged index modulation area could be produced by a single laser pulse, leading to a strong Bragg resonance in the sapphire fiber, and an SFBG with a reflectivity of 2.3% and a grating length of 2 mm was fabricated based on these filament tracks with a very short fabrication time of merely ∼1.1 s. Moreover, a WDM SFBG array, including five SFBGs, was efficiently constructed, and the SFBG array assembled by the filament tracks can operate at a very high temperature of 1600°C. These results show that the femtosecond laser filaments are very suitable for efficient production of SFBG arrays, which could be developed for quasi-distributed high-temperature sensing in many applications, such as power stations and aerospace industries.

Funding. National Natural Science Foundation of China (61875128, 62005170, 91860138); Guangdong Science and Technology Department (2019TQ05X113, 2019A1515111114, 2019B1515120042); Science and Technology Planning Project of Shenzhen Municipality (RCYX20200714114538160, JCYJ20180507182058432, JCYJ20200109114201731); China Postdoctoral Science Foundation (2019M663049).

Disclosures. The authors declare no conflicts of interest.

Data Availability. Data underlying the results presented in this paper are not publicly available at this time but may be obtained from the authors upon reasonable request.

REFERENCES

1. D. Grobnic, S. J. Mihailov, C. W. Smelser, and H. M. Ding, IEEE Photonics Technol. Lett. **16**, 2505 (2004).
2. C. Chen, X. Y. Zhang, Y. S. Yu, W. H. Wei, Q. Guo, L. Qin, Y. Q. Ning, L. J. Wang, and H. B. Sun, J. Lightwave Technol. **36**, 3302 (2018).
3. T. Elsmann, T. Habisreuther, A. Graf, M. Rothhardt, and H. Bartelt, Opt. Express **21**, 4591 (2013).
4. S. Yang, D. Hu, and A. B. Wang, Opt. Lett. **42**, 4219 (2017).
5. X. Z. Xu, J. He, C. R. Liao, K. M. Yang, K. K. Guo, C. Li, Y. F. Zhang, Z. B. Ouyang, and Y. P. Wang, Opt. Lett. **43**, 4562 (2018).
6. X. Z. Xu, J. He, C. R. Liao, and Y. P. Wang, Opt. Lett. **44**, 4211 (2019).
7. A. Brodeur, C. Y. Chien, F. A. Ilkov, and S. L. Chin, Opt. Lett. **22**, 304 (1997).
8. W. Liu, S. L. Chin, O. Kosareva, I. S. Golubtsov, and V. P. Kandidov, Opt. Commun. **225**, 193 (2003).
9. K. Yamada, W. Watanabe, T. Toma, and K. Itoh, Opt. Lett. **26**, 19 (2001).
10. Amina, L. F. Ji, T. Y. Yan, Y. H. Wang, and L. Li, Opt. Laser Technol. **116**, 232 (2019).
11. A. Benayas, D. Jaque, B. McMillen, and K. P. Chen, Opt. Express **17**, 10076 (2009).
12. A. Benayas, D. Jaque, B. McMillen, and K. P. Chen, J. Appl. Phys. **107**, 033522 (2010).
13. M. Bernier, S. Gagnon, and R. Vallee, Opt. Mater. Express **1**, 832 (2011).
14. A. Saliminia and R. Vallee, Opt. Commun. **324**, 245 (2013).
15. E. Ertorer, M. Haque, J. Z. Li, and P. R. Herman, Opt. Express **26**, 9323 (2018).
16. R. DeSalvo, A. A. Said, D. J. Hagan, E. W. Van Stryland, and M. Sheik-Bahae, IEEE J. Quantum Electron. **32**, 1324 (1996).